Nature of the smectic F phase

J. J. Benattar, J. Doucet, M. Lambert, and A. M. Levelut
Laboratoire de Physique des Solides associé au Centre National de la Recherche Scientifique, Université Paris-Sud—Bâtiment 510, 91405 Orsay, France
(Received 12 February 1979; revised manuscript received 24 May 1979)

X-ray diffraction patterns of single-domain samples of the smectic F phase of terephthalydene-bis-4-n-pentylaniline, obtained by melting single crystals of the crystalline phase, have enabled us to collect important information concerning the nature of this phase. The smectic layers are almost uncorrelated, and within the layers the order is characterized by a pseudohexagonal order analogous to that observed in the smectic B phase with tilted molecules, but less well defined: the smectic F phase is intermediate between the smectic B and smectic C phases. An intensity profile analysis performed on single-domain patterns is consistent with the two-dimensional structure of the smectic F phase, and the investigation of the powder pattern indicates in addition the existence of another disorder type which remains to be determined.

I. INTRODUCTION

Among the various mesogenic compounds only a few exhibit a smectic F phase. This phase, since its identification from miscibility criteria by Demus *et al.*,[1] has remained somewhat elusive.

Recently, Goodby and Gray synthesized several compounds in which a smectic F phase appears[2,3] and revealed the presence of such a phase in the compound TBPA (terephthalydene-bis-4-n-pentylaniline).[4] We thought it would be of special interest to study this compound since it is an homolog of the well-known TBBA (terephthalydene-bis-4-n-butylaniline) (Ref. 5) from which it only differs by the aliphatic terminal chains (butyl in TBBA, pentyl in TBPA). Therefore, it is not surprising that the polymorphism of TBPA is similar to that of TBBA, but it also shows an extra feature, the S_F phase:

$$\mathrm{Cr} \xrightarrow{76.5^\circ\mathrm{C}} S_H \xrightleftharpoons{144^\circ\mathrm{C}} S_F \xrightleftharpoons{153.5^\circ\mathrm{C}} S_C \xrightleftharpoons{182.5^\circ\mathrm{C}} S_A \xrightleftharpoons{213.5^\circ\mathrm{C}} N \xrightleftharpoons{232.5^\circ\mathrm{C}} I.$$
$$\mathrm{Cr} \nwarrow \swarrow^{57^\circ\mathrm{C}} S_G$$

[The smectic H phase (S_H in our notation) is named SmH by Goodby *et al*; but its structure is actually the same as the structure of the tilted S_B phase of TBBA which is sometimes named SmB_C. The same remark also applies to the so-called SmG phase of TBPA, which presents the same structure as that of the tilted S_E phase of TBBA (sometimes called SmE_C).]

Leadbetter *et al.*[6] have recently reported some results about the structural aspect of the S_F of this compound; from x-ray patterns obtained with samples oriented by a magnetic field, they suggested the existence of hexagonal packing within the layers. In order to study this phase in a more straightforward way, we successfully grew good single crystals of TBPA which give single domains by melting. These samples enabled us to complete Leadbetter's study; in addition we present here an analysis of the intensity profiles, which provides valuable information as regards the nature of the S_F phase.

II. EXPERIMENTAL PROCESSES

A. Preparation of samples

The single crystals of TBPA were grown in the dark in a solution of ethanol and chloroform by evaporation of the solvents over a period of about 20 days; the single crystals grown by this method are transparent and yellow, and have a platelike morphology and a parallelepiped shape with typical dimensions of the order of 10×0.5 mm.[2]

B. Experiments

The x-ray patterns of single domains were taken by means of a transmission device with a monochromatic convergent beam (Cu$K\alpha$, 1.54Å) perpendicular to a flat film. The sample is fixed, and held at temperatures within ± 0.5°C. From various S_H phase patterns, we have deduced the orientation of the long molecular axes $\vec{c}$ with respect to the external faces of the samples. We observe that the orientation of TBPA molecules differs from one sample to another: the layer planes are not always parallel to the larger external faces. We have represented in Fig. 1(A) the two geometries A and B used in x-ray experiments; they allow, respectively, examination of the $(\vec{a}^*, \vec{c}^*)$ and $(\vec{a}^*, \vec{b}^*)$ reciprocal planes. [The $\vec{a}$ and $\vec{b}$ axes are chosen in the smectic layer plane as shown in Fig. 1(B)].

Powder patterns were recorded with a Guinier camera equipped with an electric stage and using a focused monochromatic beam (Co $K\alpha_1$, 1.789Å).

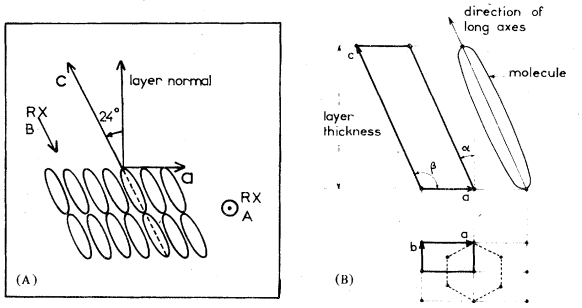

FIG. 1. (A) The two orientations A and B of the x-ray beam with respect to the long molecular axis ($\vec{c}$) and the smectic layers. (B) S_H lattice orientation with respect to the smectic layers [the plane ($\vec{a}$, $\vec{b}$) is parallel to the smectic layers].

This device permits us to obtain lattice constants in the ordered smectic phases and the layer thickness in all the smectic phases.

III. EXPERIMENTAL RESULTS

A. S_H phase

The two x-ray patterns of the S_H phase of TBPA [Figs. 2(A), 2(B)] are typical of a S_H phase, with molecules tilted by an angle α relative to the layer normal; they are quite similar to the homologous patterns of TBBA.[7-9]

i. When the direct beam is almost parallel to the smectic layers (geometry A) the corresponding pattern [Fig. 2(A)] exhibits different Bragg reflections: the very sharp $00l$ spots [Fig. 2(A),(a)], the $hk0$ spots—characteristic of the order within the layers—and hkl spots ($l = \pm 1, \pm 2$) [Fig. 2(A),(b)]. The $hk0$ and hkl reflections are in fact located along arcs of a circle, which in that kind of sample is usual; this phenomenon is indicative of a disorientation of the normal direction to the smectic layers up to 20°, whereas it is less than 5° in TBBA. The most significant point is that these reflexions are as sharp as those usually observed with crystalline phases. This is quite clear on the powder patterns of the S_H phase which exhibit very sharp rings as in the TBBA case.[7] The existence of sharp hkl ($l = \pm 1, \pm 2$) reflections is indicative of a three-dimensional order.

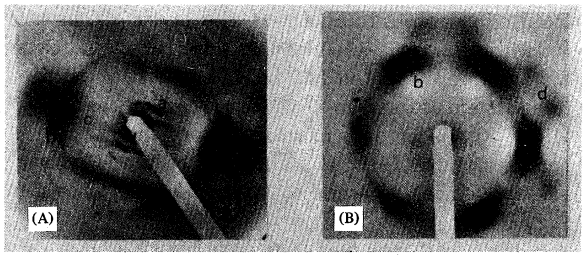

FIG. 2. X-ray patterns of the S_H phase. (a) in geometry A: (a) designates $00l$ Bragg spots, (b) hkl Bragg spots, and (c) the diffuse sheets. (b) in geometry B: we can clearly see the pseudohexagonal packing (d) designates the diffuse spots.

The pattern also shows diffuse equidistant parallel lines [Fig. 2(A), (c)], which are the traces on the film of diffuse sheets parallel to the ($\vec{a}^*$,$\vec{b}^*$) reciprocal plane. This effect results from the x-ray diffraction by periodic chains of molecules oriented along $\vec{c}$; the molecular longitudinal displacements are correlated along one chain but not from one chain to another. It may be noticed that such a description in terms of collective longitudinal displacements along chains is completely consistent with the three-dimensional order of the structure; another equivalent description of the same effect would be to introduce soft phonons polarized along the molecular direction and having their wave vectors parallel to the ($\vec{a}^*$,$\vec{b}^*$) reciprocal plane; the resulting molecular displacements would be correlated only in the chain direction. These "undulation modes"[8] are compatible with the concept of layers correlated in a three-dimensional lattice. Such an effect is related to the large anisotropy of the thermal motion of the molecules (~2-Å amplitude in the $\vec{c}$ direction), the mean positions of these molecules being distributed on the three-dimensional lattice which is defined below.

ii. When the direct beam is parallel to the long molecular axes (geometry B), the pattern [Fig. 2(B)] exhibits six $hk0$ Bragg spots forming a pseudohexagon. We noticed again the existence of some hkl ($l = \pm 1, \pm 2$) Bragg spots close to each $hk0$ Bragg spot, the existence of which has been discussed above. Besides, the hkl spots are distributed on an arc of a circle, bearing evidence that the layers are disoriented by up to 25° (5° in TBBA); it is not possible to specify whether this disorientation occurs between neighboring layers or between stacks of layers with parallel axes.

The three-dimensional structure can be described by a C-face-centered monoclinic cell whose parameters are accurately determined from powder patterns. At (132 ± 2)°C, we find

$$a = 9.62 \pm 0.02\text{Å}, \quad b = 5.14 \pm 0.01\text{Å},$$

$$c = 31.2 \pm 0.2\text{Å}, \quad \beta = 113.6 \pm 0.5°,$$

which gives a tilt angle of 23°6′ [Fig. 1(B)].

Finally, the presence of twelve diffuse spots located outside the $hk0$ Bragg spots [Fig. 2(B),(d)] is indicative, as for the S_B phase of TBBA, of a local "herringbone packing" of the molecular sections within the layers, inside small domains whose size is here or the order[9] of 20–30 Å.

B. S_F phase

(i) When the direct beam is parallel to the smectic layers (geometry *A*), the x-ray pattern of this phase [Fig. 3(A)] appears to be different from the S_H one. Indeed, the diffuse sheets observed in the S_H phase have, in this case, almost vanished, the *hk*0 Bragg spots are now transformed into diffuse peaks, and the *hkl* Bragg spots have then disappeared. These phenomena are indicative of the loss of three-dimensional order: the smectic layers are now very weakly coupled.

(ii) We can observe in Fig. 3(B), where the direct beam is parallel to the long molecular axes (geometry *B*), that the x-ray pattern, characteristic of the order within the layers, presents a diffuse ring whose intensity is modulated with maxima arranged in six diffuse peaks at the same place as the *hk*0 spots of the S_H phase. The intensity distribution evokes a hexagonal packing similar to that of the S_H phase, but far less well defined. Nevertheless, this intensity distribution is clearly indicative of the persistence of *some orientational correlation* between layers.

Another interesting feature can be seen on the original pattern corresponding to Fig. 3(B)(g): the intensity of the twelve previous diffuse spots of the S_H phase is uniformly distributed around the diffuse ring, thus indicating the persistence of a local herringbone packing.

The Debye-Scherrer patterns yield less information about the S_F phase than the S_H phase since they only exhibit a diffuse ring instead of sharp rings at large diffraction angles. Consequently, no accurate cell dimensions can be given; from the analysis of single domain patterns [Figs. 3(A) and 3(B)], we can only state that the local cell parameters are roughly the same as in the S_H phase. And on that point, we disagree with the results of Leadbetter *et al.*,[6] which report accurate cell parameter values for the S_F phase.

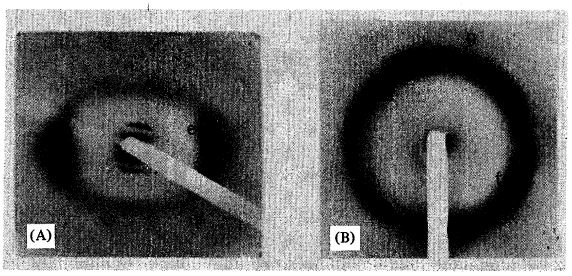

FIG. 3. X-ray patterns of the S_F phase. (A) in geometry *A*, the diffuse sheets almost vanished and the *hk*0 Bragg spots are transformed into diffuse peaks (e). (B) in geometry *B*, the diffuse ring is modulated by intensity maxima (f), and the diffuse spots (d) give the intensity (g) distributed around the ring.

Indeed, such values cannot be calculated with precision from the x-ray patterns, which only exhibit broad reflections, excepting the 00*l* reflections.

The only accurate deduction we can make from the powder patterns of the S_F phase is the layer thickness *d*. Assuming that the molecular length *l* remains equal to the length of the *c* parameter measured in the S_H phase (31.2 Å at 132 °C), we can infer the tilt angle α, which is given by the formula $d = l\cos\alpha$. We obtain

$d = 28.6 \pm 0.2$Å, $\alpha = 23.6 \pm 1°$ (S_H, 132°C),

$d = 29.4 \pm 0.2$Å, $\alpha = 20 \pm 1°$ (S_F, 150°C),

$d = 30.9 \pm 0.2$Å, $\alpha = 8 \pm 3°$ (S_C, 155°C).

These values show that the S_F is also an intermediate state between the S_H and the S_C phase as regards the tilt angle.

IV. INTENSITY PROFILES

A. Single-domain patterns

It proved to be impossible to analyze in the S_H phase the diffuse scattering around the *hk*0 reflections because, on account of the disorientations within the sample (cf. Sec. IIA i), *hkl* reflections appear around the *hk*0 reflections; nevertheless, it is very probable that the diffuse scattering intensity varies as in the TBBA case, where longitudinal phonons can propagate[10]; i.e., this intensity $I(\vec{q})$ is such that $I(\vec{q}) \propto |q|^{-2}$, with $\vec{q} = \vec{S} - \vec{\tau}$ (where $\vec{S}$ is the scattering vector parallel to $\vec{\tau}$ and $\vec{\tau}$ a reciprocal lattice position).

In contrast, such an analysis *is* possible in the S_F phase. We tried to fit its intensity profile with a function such as $|q|^{-x}$ (here $\vec{q}$ is parallel to $\vec{\tau} = 2\vec{a}^*$), and we obtained $x = 1.50 \pm 0.05$. This result only indicates that the S_F phase behaves quite differently from that of $S_H(S_{B_C})$. The value $x = 1.50$ is only suggestive, since no deconvolution has been done from the intrinsic instrumental line shape and the sample mosaics. The instrumental resolution is sufficiently good to have no measurable effect on the linewidth for a three-dimensional ordered crystal. If we assume a two-dimensional order (uncorrelated layers), the sample mosaics combined with the two-dimensional features of the scattering, which consists of rods perpendicular to the $(\vec{a}, \vec{b})$ plane, will contribute a large part of the measured width and is difficult to take into account quantitatively. Since we did not succeed in preparing a better-oriented sample, powder experiments were then performed in order to simplify the analysis of the intensity profile.

In the above discussion, we did not consider that optical modes can contribute to the diffuse scattering. We have assumed this contribution as

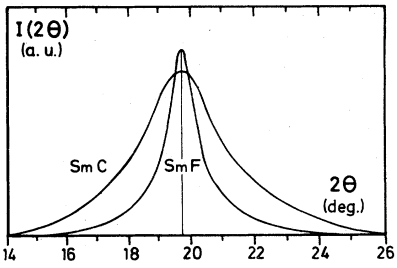

FIG. 4. Comparison of the intensity profiles between the S_F and S_C phases ($\lambda = \text{Cu } K\alpha$).

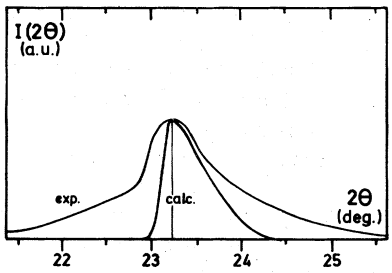

FIG. 5. The experimental and calculated intensity profiles of the diffuse ring on powder diagrams in the S_F phase ($\lambda = \text{Co } K\alpha$).

a negligible one since we do not think that low-frequency optical modes exist in the S_F phase; this had been checked through neutron experiments in the S_H phase of TBBA,[10] and we assume that this is also the case in the S_F phase of TBPA.

It is also interesting to compare the intensity profiles of the S_F and S_C phases (Fig. 4). The intensity profile of the S_F phase is less broad and less homogeneous than in the S_C phase [the angular widths at midheight are, respectively, $\Delta(2\theta)_F = 1°$ and $\Delta(2\theta)_C = 3°$]. This finding corroborates the preceding ones concerning the intermediate nature of the S_F phase between the S_H and S_C phases.

B. Powder patterns

Powder patterns of the S_F phase exhibit only two sharp reflections (001 and 002) at small angles and a broad diffuse ring at large angles. We have calculated its theoretical intensity profile, assuming a complete disorder between parallel layers and a perfect long-range order within the layers in order to see if the lack of correlation between layers is the only phenomenon which is responsible for the broadening of the ring.

Under such assumptions, the intensity is localized in reciprocal space along bars, parallel to $\vec{c}^*$ whose length[11] is about $2/C$ Å^{-1}. The electronic density is chosen such that

$$\begin{cases} \rho(x) = 1 & \text{for } -C/2 \leq x \leq C/2\,, \\ \rho(x) = 0 & \text{elsewhere.} \end{cases}$$

The intensity along the bars is therefore given by the square of the Fourier transform:

$$I(q) \propto c^2(\sin\pi qc/\pi qc)^2\,;$$

the intensity of the diffuse ring $I(2\theta)$ is then obtained by means of a graphic method, summing the intensity projections of the 110 and 200 bars on the 2θ axis.[12] This theoretical profile is compared with the experimental one in Fig. 5. We can see that its width at midheight is about two times smaller than the experimental one, which implies that the disorder responsible for the broadening of the ring at large diffraction angles cannot be described roughly merely by the lack of correlation between the layers; it involves extra disorder phenomena probably corresponding to a loss of the long-range order within the layers or to lattice-dynamic effects. From our x-ray experiments we cannot distinguish between the two possibilities; further experiments, such as neutron experiments, are required to determine the true nature of this extra disorder.

It is worthwhile to compare the powder diagrams of the S_F phase of TBPA with that of the SmIII phase of HOBACPC, which is a ferroelectric compound exhibiting a similar stacking of uncorrelated layers[13]; the two patterns show a diffuse ring at large diffraction angles, but the SmIII diffuse ring is sharper than that of S_F, which indicates that the lateral hexagonal order within the layers extends to longer distances and is better defined in the SmIII phase than in the S_F phase.

V. CONCLUSION

As do all the other smectic phases (except the S_D phase), the S_F phase of TBPA presents a clearly defined layered structure indicated by the sharpness of the $00l$ Bragg spots. At large diffraction angles, the patterns only exhibit one diffuse broad ring whose intensity is modulated into six maxima, which are reminiscent of the pseudo-hexagonal structure of the ordered smectic phases. Thus the structure of the S_F phase appears to be intermediate between the structure of the S_C phase (liquid order) and the structure of the S_B phase. We found that one of the relevant features of the S_F phase is the nearly complete absence of positional correlation between successive layers, while some orientational correlation is retained. We have to deal with a two-dimensional structure with regard to the positional order of molecules, whereas the other ordered smectic phases are characterized by three-dimensional order. In such conditions, the de Gennes–Sarma model[14], which had

been formerly proposed for the structural description of the S_B phase, seems to be more appropriate for the S_F phase. From our experiments, it is difficult to ascertain whether the loss of the three-dimensional order is accompanied by a loss of the long-range order within the layers or by some kind of molecular motion. It is worth noting that the $S_H - S_F$ transition which corresponds to the transformation of the three-dimensional order into two-dimensional order is discontinuous, since this transition is a first-order one.

While this work has clarified some of the essential properties of the S_F phase, it leaves unanswered the question as to what factors influence its formation. Further investigations on the nature and behavior of the S_F phase are needed before these factors can be ascertained.

ACKNOWLEDGMENTS

We are very grateful to Dr. C. Germain for synthesizing the compound TBPA and to Mrs. M. C. Comes for revising the English manuscript.

[1]D. Demus, S. Diele, M. Klapperstück, V. Link, and H. Zaschke, Mol. Cryst. Liq. Cryst. 15, 161 (1971).
[2]J. W. Goodby and G. W. Gray, Mol. Cryst. Liq. Cryst. 41, 145 (1978).
[3]J. W. Goodby, G. W. Gray, and A. Mosley, Mol. Cryst. Liq. Cryst. 41, 183 (1978).
[4]S. Sakagami, A. Takase, and M. Nakamizo, Mol. Cryst. Liq. Cryst. 36, 261 (1976).
[5]J. Doucet, J. P. Mornon, R. Chevalier, and A. Lifchitz, Acta Crystallogr. B 33, 1701 (1976); J. Doucet, A. M. Levelut, and M. Lambert, *ibid.* 33, 1710 (1976).
[6]A. J. Leadbetter, J. P. Gaughan, B. Kelly, G. W. Gray, and J. Goodby, in Proceedings of the International Conference on Liquid Crystals, Bordeaux, 1978, J. Phys. (Paris) 40, C3, 178 (1978).
[7]J. Doucet, A. M. Levelut, and M. Lambert, Phys. Rev. Lett. 32, 301 (1974).
[8]W. Helfrich, in Ref. 6; J. Phys. (Paris) 40, C3, 105 (1979).
[9]A. M. Levelut, J. Phys. (Paris) Colloq. C3-37, C-51, (1976).
[10]J. Doucet, M. Lambert, A. M. Levelut, P. Porquet, and B. Dorner, J. Phys. (Paris) 39, 173 (1978); J. J. Benattar, A. M. Levelut, L. Liebert, and F. Moussa, J. Phys. (Paris) 40, C3, 115 (1978).
[11]A. Guinier, *X-Ray Diffraction* (Freeman, San Francisco, 1963).
[12]A. Tardieu, V. Luzzati, and F. C. Reman, J. Mol. Biol. 75, 711 (1973).
[13]J. Doucet, P. Keller, A. M. Levelut, and P. Porquet, J. Phys. (Paris) 39, 548 (1978).
[14]P. G. de Gennes and G. Sarma, Phys. Lett. A 38, 219 (1972).

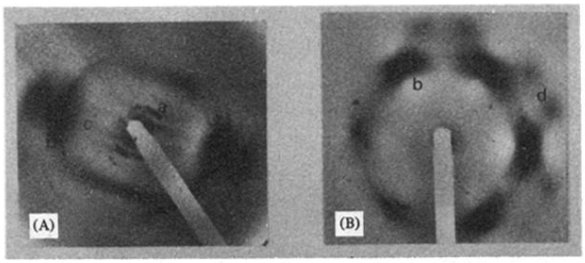

FIG. 2. X-ray patterns of the S_H phase. (a) in geometry A: (a) designates $00l$ Bragg spots, (b) hkl Bragg spots, and (c) the diffuse sheets. (b) in geometry B: we can clearly see the pseudohexagonal packing (d) designates the diffuse spots.

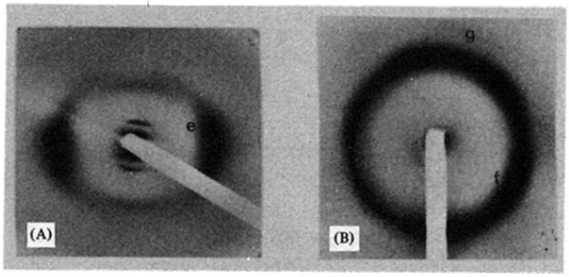

FIG. 3. X-ray patterns of the S_F phase. (A) in geometry A, the diffuse sheets almost vanished and the $hk0$ Bragg spots are transformed into diffuse peaks (e). (B) in geometry B, the diffuse ring is modulated by intensity maxima (f), and the diffuse spots (d) give the intensity (g) distributed around the ring.